Dynamic Film Boiling on Moving Steel Plates: Insights from Computational Fluid Dynamics for Industrial Heat Transfer Optimization

[1]Sushil Kumar, [2]Dr. Sohail Bux
[1]M.Tech Scholar, [2]Professor,
[1]Department of Mechanical Engineering, Agnos College of Technology, Bhopal (M.P)
[2]Department of Mechanical Engineering, Agnos College of Technology, Bhopal (M.P)
Email-: [1]su999kumar@gmail.com, [2]buxsohail@gmail.com

* Corresponding Author: Sushil Kumar

Abstract: *In industrial heat transfer operations, film boiling is a crucial occurrence, especially in applications like plate cooling in the steel industry, where effective heat dissipation directly affects manufacturing efficiency and product quality. This work represents the dynamics of film boiling on a moving steel plate by considering complicated interactions of varied heat transfer properties at different velocities of the plate using computational fluid dynamics. The Volume of Fluid (VOF) model is used to simulate the Multiphase flow and gain complete information regarding the interaction between the liquid water phase and vapor phases on the plate surface. Some of the major results throwing new light on key variables like heat flow, Nusselt number, and temperature profile at plate speed 0.1, 0.2, and 0.5 m/s are given here. One of the interesting observations is that with an increase in plate velocity, there is actually a slowing-down of the mixture's convection heat transfer coefficient. This will have important bearing on the fluid dynamics role in film boiling conditions toward efficiency in the heat transfer process since this result shows a reduction in the overall efficiency in dissipating heat at higher speeds.*

Moreover, in the phase-specific analysis on heat fluxes and mass flow rates for liquid and vapor phases under dynamic conditions, very distinct patterns come about. Results point out that, indeed, film boiling is a pretty complex process wherein dramatic changes in heat transfer mechanisms are strongly conditioned by the dynamic interaction among the cooling media and the moving plate. Knowledge of these dynamics is key to maximizing cooling strategies tailored for specific industrial applications, thus increasing process efficiency and the quality of manufactured products in many areas

Keywords: *Film Boiling, Steel Plate Cooling, Computational Fluid Dynamics, Heat Transfer, Multiphase Flow, Nusselt Number, Heat Flux.,*

I. INTRODUCTION

Film boiling is one of the important phenomena of various heat transfer areas that, in particular, apply to plate cooling processes of steel production. Plate cooling, as one of the very important processes in the manufacturing of steel, significantly affects the mechanical properties of the final product. Various cooling methods that are used to attain specified cooling rates include circular impinging water jets, slit impinging water jets, mist cooling, and air cooling. Studies on the circular impinging water jet method are very widespread due to its great ability to manage the intricate dynamics of multiphase flows and phenomena associated with phase-change heat transfer [1]–[5].

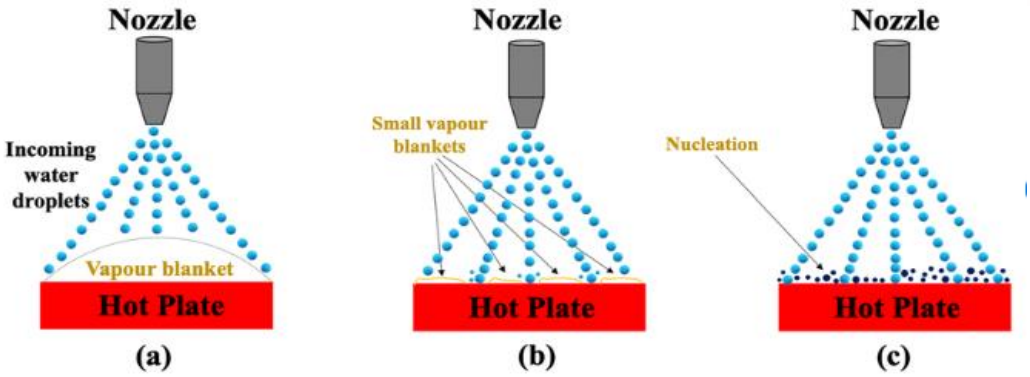

Figure 1. (a) Film Boiling (b) Transition Boiling (c) Nucleate Boiling [6]

In plate cooling, the process where cooling water interacts with a heated steel plate involves phenomenon known as film boiling. During this process, a layer of vapor forms between the water and the hot plate. This vapor layer significantly impacts the heat transfer rate, acting as an insulating barrier that reduces the overall efficiency of heat removal. The process is further complicated by the high-speed movement of the steel plate, which affects the behavior of the water on the plate's surface. The dynamic interaction between the motion plate and the cooling water introduces additional complexities, as it involves a moving interface that is thermally coupled with the plate and the water. Solving this

problem requires a comprehensive understanding of the temperature and heat flux distribution on the plate, which can only be determined through detailed calculations that account for the intricate physics involved in the film boiling process [5]. This makes film boiling a significant phenomenon to study and optimize in the context of enhancing the efficiency and effectiveness of industrial cooling processes as shown in figure 1.

A. Concept of heat transfer through boiling:

In many applications, boiling heat transfer depends in fact upon fluid properties of a critical nature, such as density, ρ, viscosity, μ, thermal conductivity, k, and specific heat capacity, c_p. These are essentially the major parameters that will allow one to estimate what extent heat conducts within the liquid and across the liquid-vapor interface. Surface tension, σ, together with the aforementioned parameters, exerts a controlling influence on bubble formation and dynamics by determining the energy required in creating new surface area at the liquid-vapor interface.

The surface tension may form bubbles in the liquid-vapor interface, whereby the molecules are attracted towards the liquid phase. If a solid surface heats adjacent liquid above its saturation temperature, then vapor bubbles initiate and start expanding. Such expanding bubbles are influenced by temperature and corresponding pressure differences between the vapor inside the bubble and surrounding liquid [6]–[9]. Heat transfer occurs either from the bubble to the cooler liquid, thus condensing and collapsing it, or from the liquid at a higher temperature into the bubble, thus expanding it and letting it rise buoyantly.6 Mechanisms which control boiling heat transfer must be understood to enable optimization of systems in industry—from power generation to cooling systems—the behavior of which requires nuanced consideration of fluid dynamics and material properties. Based on the existence of bulk fluid motion, boiling may be classified as pool boiling or flow boiling. This has been shown in Figure 2.

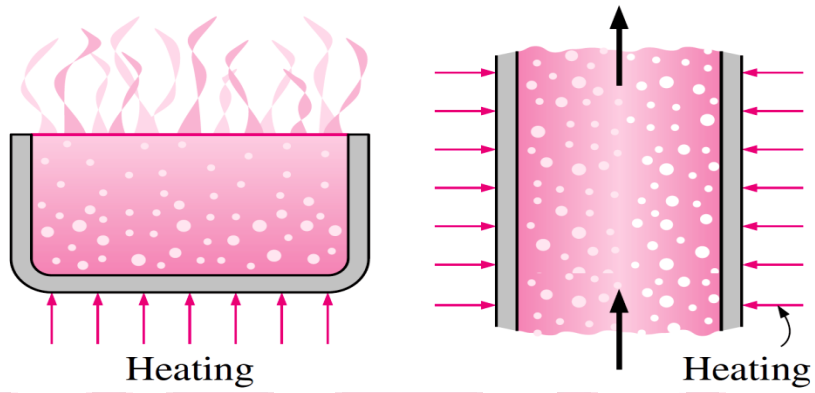

Figure 2. Dividing boiling according to whether bulk fluid motion is present. Pool boiling (a) and flow boiling (b).

B. Boiling Curve and Boiling Regimes

Four distinct boiling regimes are identified: nucleate boiling, film boiling, transition boiling, and natural convection boiling. Figure 3. illustrates a boiling curve that plots the boiling heat flow against the excess temperature, depicting these regimes. Although this particular curve is for water, its general shape is consistent for other fluids. The exact form of the curve depends on the combination of the heating material and the fluid pressure, while the geometry of the heating surface has minimal impact. We will discuss each boiling regime in great detail [1], [10], [11].

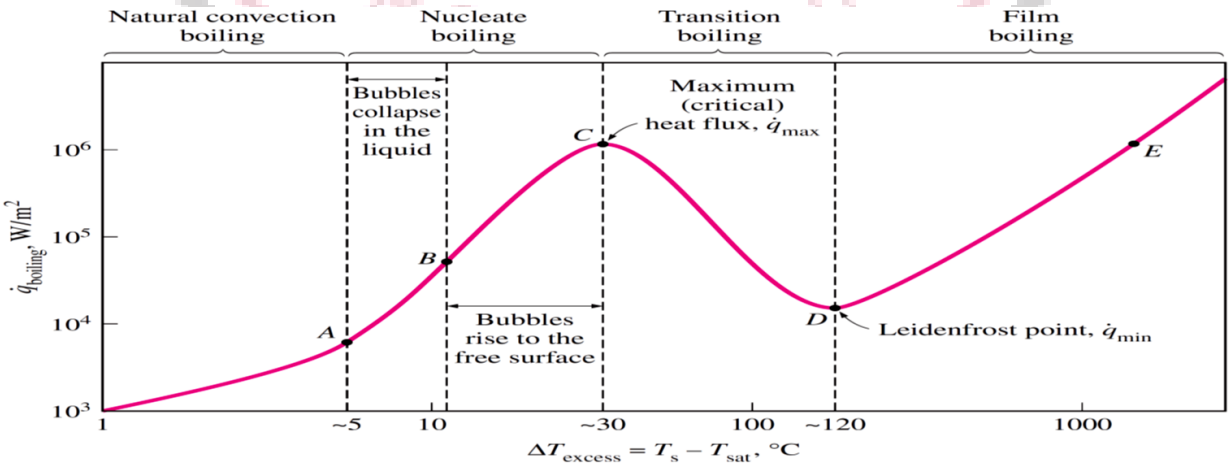

Figure 3. Normal water boiling curve at one atmosphere of pressure[7]

C. Achieving Point A on the Boiling Curve via Natural Convection

In practical applications, pure substances generally start to form bubbles upon reaching their saturation temperature at a specific pressure. However, in real-world scenarios, bubbles may not form on the heating surface until the liquid has been heated a few degrees beyond this saturation temperature—typically around 2 to 6°C higher for water. This phenomenon indicates that the liquid is somewhat superheated, existing in a metastable state until it reaches the boiling point where bubbles can form freely on the surface. During this process, heat transfer from the heating surface to the fluid is primarily facilitated by natural convection, driven by convection currents within the liquid.

D. Boiling should begin at point (A–C).

In the nucleate boiling regime, bubbles initially form at point A on the boiling curve, emerging at specific nucleation sites on the heated surface. As we move towards point C, more bubbles emerge at an increasing number of nucleation sites. This regime can be split into two distinct zones: A-B and B-C. In zone A-B, individual bubbles emerge at favored nucleation sites on the heated surface and rapidly dissolve back into the liquid after detachment. This cycle repeats as liquid flows in to replace the rising bubbles. Enhanced heat transfer coefficients in this phase are primarily due to the turbulence and agitation induced by the liquid moving towards the heater surface. In zone B-C, as the heater temperature rises further, bubbles form rapidly and plentifully across numerous nucleation sites, creating continuous columns of vapor that rise to the liquid's free surface and burst. The combination of evaporation and liquid movement toward the surface results in significantly high heat fluxes achievable in this region of the boiling process [12]–[16].

When the evaporation rate of the heater's surface reaches high levels at large values of 〖ΔT〗_excess, it becomes challenging for the liquid to reach and wet the heater surface. A considerable portion of the heater surface has been covered with bubbles. When a result, when 〖ΔT〗_excess grows, the heat flux elevates more slowly and reaches its optimum level at point C. The heat flow at this location is known as (q_max)˙, which stands for critical (or maximum) heat flux. The essential heat flux for water is more than 1 MW/m2

E.Significance and contribution of film boiling

The significance and contribution section of a research project or study serves to delineate the distinctive aspects and implications of the research findings. Its primary goal is to underscore how the study enriches the current knowledge base within the field and addresses existing gaps or challenges.

Firstly, it emphasizes the novelty and originality of the research, highlighting any novel methods, approaches, or insights that advance understanding in the field. Secondly, it identifies specific issues or questions within the discipline that the research endeavors to tackle, potentially offering new solutions or perspectives. Thirdly, it explores the impact of the findings on both theoretical frameworks and practical applications within the field, potentially paving the way for the development of new hypotheses or paradigms. Lastly, the section highlights any comparative advantages or unique aspects of the study in relation to prior research, underscoring its potential to influence future studies or applications. Together, these elements provide a comprehensive overview of how the research contributes to advancing knowledge and fostering innovation within its respective field.[9]

II. LITERATURE REVIEW

Liu, X. et al. (2022) [10]: Liu et al. developed a conceptual framework for bubble nucleation in liquid film boiling, considering factors like superheating requirements, transient heat conduction facilitated by a porous wick, and evaporation at the liquid-vapor interface. Their study establishes criteria for the onset of nucleate boiling (ONB) in liquid film boiling, demonstrating that micro-cavities for bubble nucleation are more narrowly distributed compared to pool boiling. They found that a super-hydrophilic surface with a small contact angle can hinder bubble formation, thereby facilitating ONB at smaller micro-cavity radii. Experimental results corroborate their theoretical predictions, providing insights for future design upgrades in liquid film boiling systems.

Langmuir (2022) [17]: Langmuir investigates nano-scale thin film boiling on heterogeneous surfaces using non-equilibrium molecular dynamics modeling. They observe superior heat and mass transfer performance in nano-scale thin-film boiling due to internal fluid flow dynamics and the triple-phase interface intricacies. Their findings show that surface roughness enhances efficiency and delays steady boiling onset, achieving high heat flux and heat transfer coefficients on hydrophilic surfaces. Conversely, hydrophobic surfaces degrade heat transfer due to vapor layer entrapment. Langmuir's work suggests optimizing surface wettability and area percentage of hydrophilic zones to enhance heat and mass transmission efficiency in vaporization processes.

Chen, G. et al. (2023) [18]: Chen et al. propose a novel heat sink design utilizing liquid film boiling within a hybrid mesh structure with an active liquid supply. Their design achieves high thermal flux and mean heat transfer coefficients using water under atmospheric conditions, with minimal pumping power and water consumptionThe key innovation utilizes its highly hydrophilic porous layer to enable efficient liquid film boiling, which optimizes heat dissipation for two-phase cooling applications. Theoretical models and visualizations prove that the escape of vapor bubbles controls the limits of thermal fluxes, guaranteeing long-lasting high-performance cooling under challenging conditions.

Kim, K. M. et al., 2022 [19]**:** Kim et al. propose physics-informed machine learning frameworks for the prediction of minimum film boiling temperature under different scenarios. It merges machine learning techniques with physics-based models to improve TMFB prediction accuracy beyond traditional empirical correlations. Random-forest algorithms were found to combine the advantages of both types of correlations previously established, such as the Groeneveld-Stewart correlation, which had maintained good performance in TMFB prediction not only for interpolation scenarios but also for extrapolation. The paper by Kim et al. enables the improvement of predictive capability on thermal and fluid behaviors in the case of a loss-of-coolant accident in light-water reactors.

Li et al. (2022): Li et al. investigate the potential of liquid-vapor phase transition heat spreaders in dispersing waste heat at compact spaces critical for microprocessors and high-power applications. In doing this, the researchers couple hierarchical mesh wicking with ultra-high thermal conductivity material to improve heat transfer through liquid film boiling. The experiments on heat removal capacity and coefficient of heat transfer are very impressive, which forecasts the effectiveness of their approach in high-flux heat spreader applications.

Khorram, A., & Mortazavi, S. (2022) [15]: Khorram and Mortazavi employ direct numerical simulations to study film bubbling dynamics on horizontal surfaces in three dimensions. Their simulations incorporate energy and momentum equations for both phases, addressing interface deformation, viscosity, and inertia effects. They investigate the impact of Grashof and Jacobs numbers on fluid flow, heat transfer, and bubble dynamics, revealing buoyancy's role in reducing viscous effects and influencing Nusselt number. Their study provides insights into optimizing surface characteristics and unit cell dimensions for enhanced heat transfer in film boiling scenarios.

III. OBJECTIVE

- This study provides practical guidelines and recommendations for addressing film boiling phenomena in steel plate production. In this setup, the steel plate's surface temperature exceeds the saturation temperature of the surrounding liquid (typically water), leading to film boiling.
- The process is marked by the periodic formation and release of steam bubbles as heat is exchanged across the vapor-liquid interface.
- The film boiling problem was simulated using the Volume of Fluid (VOF) multiphase model. Given the insufficient global research on multiphase interface mechanisms, this study focuses on the film boiling mechanism. Film boiling is commonly encountered in various applications, including metal quenching, biological species chilling, regenerative rocket cooling, cryogenic fuel tank cooling, and sometimes in nuclear reactors.
- This study is further extended by considering different saturation temperatures and varying velocities of the moving steel plate, providing a comprehensive analysis of the film boiling phenomenon under diverse conditions.

IV. METHODOLOGY

A. Cooling Mechanism of moving plates:

Figure 4. depicts the cooling mechanism used for moving plates from the finishing rolling mill, where water jets are commonly utilized due to their effective cooling capabilities.

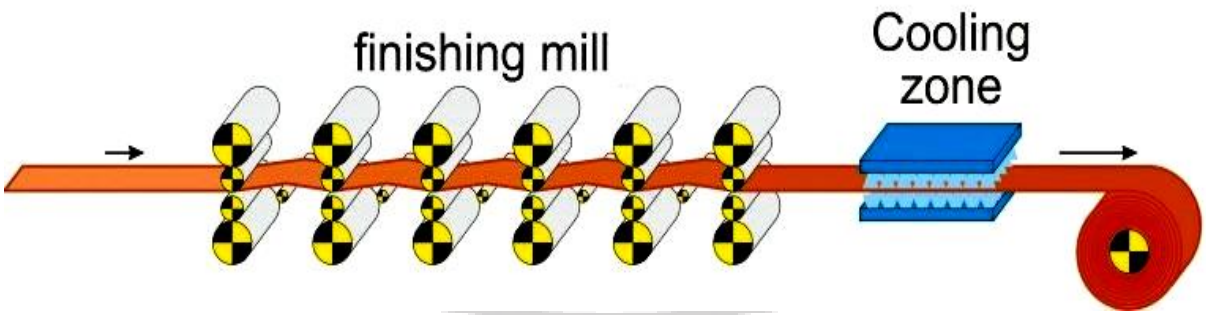

Figure 4.Cooling Mechanism of moving plates

When cooling water is applied to the moving plate, it forms a thick layer on the plate's surface. Under conditions of high flow rates, the thermal interaction between the plate and the cooling water can be categorized based on the surface temperature (Twall) of the plate.

• When the surface temperature of the plate is below the vaporization temperature of water at ambient pressure (100°C at 1 bar), the thermal interaction between the plate and the cooling water occurs without phase change. In this regime, heat transfer predominantly happens through conduction and convection processes within the water layer, without the formation of vapor bubbles or any phase transition. This mechanism is characterized by efficient heat dissipation through the cooling water, helping to maintain the plate temperature below the boiling point and ensuring stable thermal conditions.

• If the plate surface temperature surpasses 100°C but stays below the Leiden frost temperature, nucleate boiling initiates on the surface. When the surface temperature is above the Leiden frost point, a thin steam layer forms, and the mode of heat exchange between plates and cooling water changes to film boiling. High momentum within the water jet may still be adequate to break through the residual water layer and thus provide localized single-phase heat transfer in the vicinity of the impingement point on the plate surface. It is also possible that the mode of interaction between the plate and the cooling water may vary, not just with surface temperature, but also with local position on the plate. This could mean it would change from nucleate or film boiling heat transfer modes into single-phase heat transfer during its motion. This guarantees efficient cooling of the plate while it is running under varying conditions in the course of its movement.

B. CFD analysis of steel plate:

Computational fluid dynamics involves the analysis of systems of fluid flow and heat transfer using computational simulation tools. Being a versatile technique, it is applied to both industrial and non-industrial aspects. In this study, ANSYS Fluent will be used for conducting a CFD analysis to see the behavior of a moving steel plate at different velocities. The analysis incorporates basic equations, which include the Volume of Fluid model employed for multiphase flow that is combined with basic equations for continuity, momentum, and energy, together with k-epsilon turbulence equations. Numerical algorithms form the basis of solutions of fluid flow problems that CFD employs. Since the basis of such algorithms demands extensive user input, a number of developed user interfaces exist in various CFD software packages for both problem set-up and analysis of results. In view of this, three main components are involved in solving CFD problems:

1) Pre-processor,
2) Solver and
3) Post-processor.

C. Steel Plate Moving at 0.1 meters per second-CFD Analysis of Dynamic Behavior CAD geometry:

In this research, a two-dimensional CAD model of a 20 mm x 80 mm steel plate is developed using the Design module of ANSYS Workbench, as shown in Fig. 5. for its 2D view.

Figure 5. Two-Dimensional CAD Model of Steel Plate with Dimensions 20 mm x 80 mm

D. Meshing: Following the completion of the steel plate's CAD geometry, it is imported into ANSYS Workbench for subsequent computational fluid dynamics (CFD) analysis, with meshing being the next critical step. Meshing is a pivotal operation in CFD where the CAD geometry is divided into numerous small elements, known as mesh. In this study, a mesh element size of 0.1 mm is chosen shown in figure 6. The meshing process yields a total of 33,830 nodes and 33,462 quad-4 elements, each comprising four nodes and forming rectangular shapes.

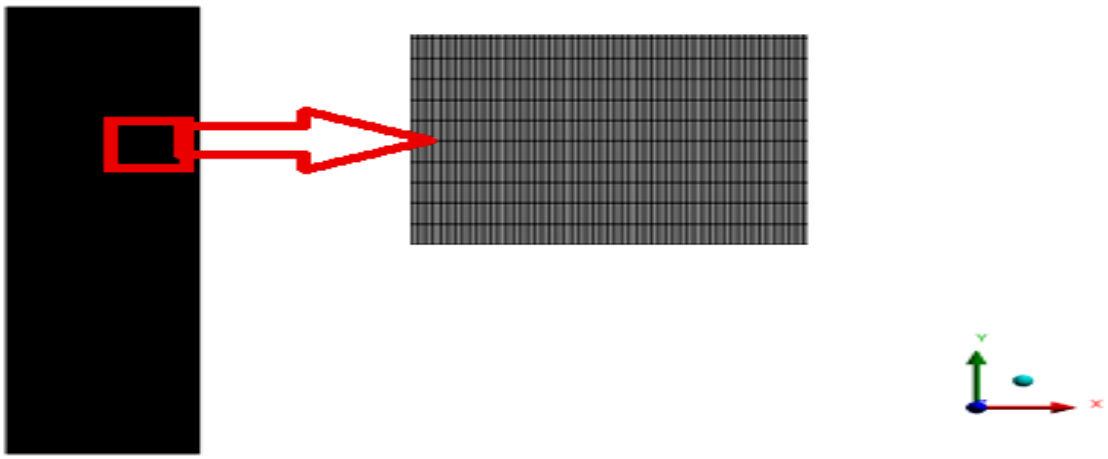

Figure 6. Mesh Generation for Steel Plate

Factors influencing mesh quality include:

- Rate of Convergence: A high-quality mesh accelerates convergence, enabling faster attainment of accurate solutions.
- Solution Precision: Improved mesh quality enhances solution accuracy, crucial for precise predictions.
- Computational Processing Time: Finer meshes increase computational demands, extending processing times.

Grid Independence: Achieving consistent fluid property results across varying mesh densities indicates grid independence, ensuring reliable simulation outcomes.

These factors underscore the importance of mesh quality in computational fluid dynamics (CFD) analyses, balancing accuracy with computational efficiency for effective engineering insights.

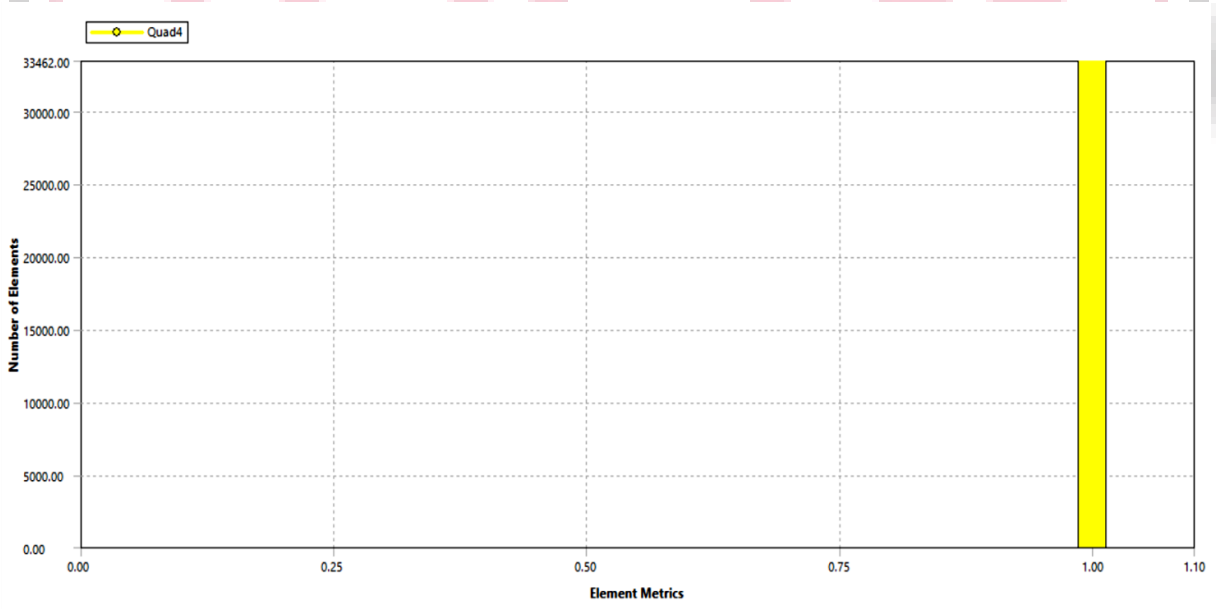

Figure 7. Mesh Orthogonality for Steel Plate

The evaluation of the orthogonality of mesh cells is done using vectors from the cell centroid to each face, corresponding face area vectors, and vectors from the cell centroid to adjacent cell centroids.(figure 7) Cells with higher orthogonality approach a value of 1, indicating better quality, whereas cells with lower orthogonality approach 0. In this study, the minimum, maximum, and average orthogonal quality values are all 1, indicating excellent and consistent mesh quality throughout. This ensures that the mesh is well-suited and optimized for accurate computational fluid dynamics (CFD) simulations of the thermal and flow characteristics of the steel plate [14], [17], [19].

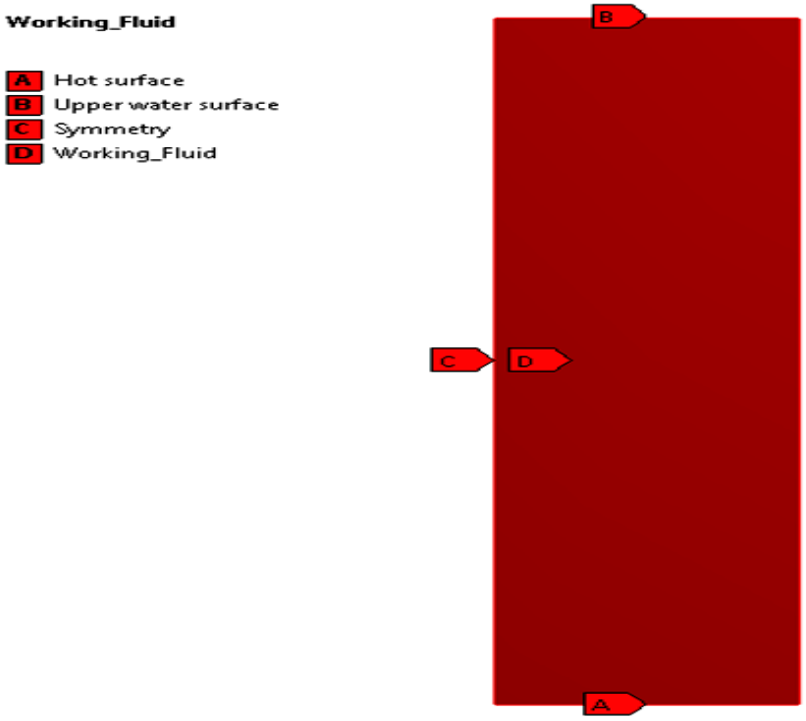

Figure 8. Various boundary conditions of the steel plate for film boiling analysis

Defining Material Properties: In ANSYS, accurately defining material properties is essential for conducting thorough analyses. If the necessary materials are not included in the ANSYS material library, users have the flexibility to create custom material databases. In this case, the fluid consists of a blend of liquid water and water vapor, while the surface material is steel. Below is an example table 1. Describing the properties:

Table 1. Describing the Material Properties

Parameter	Water liquid	Water vapor	Steel plate
Density [Kg/m3]	998.2	0.5542	8030
Specific heat (Cp) [J/kg-k]	4182	2014	502.48
Thermal conductivity (K) [W/m-k]	0.6	0.0261	16.27
Viscosity [Kg/m-Sec]	0.001003	1.34e-5	-

Here are the boundary conditions and solver settings defined for the CFD analysis:

1. Solver Configuration: Employ a transient pressure-based solver and apply gravity along the y-axis with an acceleration of -9.81 m/s².

2. Multiphase Modeling: Utilize the Volume of Fluid (VOF) method to model multiphase interactions, incorporating Implicit Body Force formulation.

3. Phase Definition: Specify vapor as the primary phase and liquid as the secondary phase.

4. Energy Equation: Activate the energy equation to compute temperature distribution across the domain.

5. Material Properties: Define the working fluid as a mixture of water (liquid and vapor), and model the steel surface with properties listed in Table 4.1.

6. Outlet Boundary Condition: Set the outlet boundary pressure to zero gauge pressure.

7. Thermal Conditions: Input a hot surface temperature of 850°C, reflecting significant superheat compared to the saturation temperature.

8. Discretization: Apply the PRESTO! Scheme for Pressure and the QUICK scheme for Momentum and Energy discretization.

9. Solver: Employ the Fluent solver to execute the computational fluid dynamics (CFD) simulations effectively.

V. RESULT AND DISCUSSION

A. Calculation of Nusselt Number, heat flux and enthalpy of the mixture:

When calculating heat transfer between a flowing fluid and a solid body, Nusselt no. is a dimensionless parameter that is utilised. It is the ratio of heat transfer across a barrier that occurs by convection as opposed to conduction. In the basic scenario, the mean fluid flow is perpendicular to the convective and conductive heat fluxes, which are parallel to one another and the boundary surface's surface normal.

$$Nu = \frac{convective\ heat\ transfer}{conductive\ heat\ transfer}$$

$$Nu = \frac{h}{K/_L} = \frac{hL}{K}$$

Where

h = convective heat transfer coefficient of the flow,

L = characteristic length

K = thermal conductive of the fluid

Selection of the characteristic length should be in the direction of growth or thickness of the boundary layer.

The thermal conductivity of the fluid is typically evaluated at the film temperature.

The mixture moving at a speed of 0.1 metres per second on the plate has the following Nusselt number:

With the mixture moving at a speed of 0.1 metres per second on the plate, the convective heat transfer coefficient is 56792.28.

$$Nu = \frac{hL}{K}$$

$$Nu = \frac{56792.28 \times 0.08}{0.6}$$

$$Nu = 7572.304$$

Nusselt number for mixture for plate moving at a speed of 0.2 meters per second:

The convective heat transfer coefficient of the mixture on the plate at a velocity of 0.2 meters per second is measured at 44854

$$Nu = \frac{44854 \times 0.08}{0.6}$$

$$Nu = 5980.533$$

Nusselt number for mixture for plate moving at a speed of 0.5 meters per second:

The convective heat transfer coefficient of the mixture on the plate at a velocity of 0.5 meters per second is measured at 35218.75

$$Nu = \frac{35218.75 \times 0.08}{0.6}$$

$$Nu = 4695.833$$

The table 2. Illustrates the Nusselt number and temperature profile of a mixture on a steel plate across different velocities: 0.1 meters per second, 0.2 meters per second, and 0.5 meters per second. It shows the Nusselt number for the mixture (including both liquid and vapor phases), with values decreasing as the speed increases. Additionally, the temperature profile of the mixture (in Kelvin) rises with higher plate velocities, indicating how heat transfer and temperature distribution vary with motion speed of the steel plate.

Table No. 2. Nusselt Number and Temperature Profile of Mixture on Steel-Plate at Varied Speeds

Table No.	**Motion of the steel- plate at 0.1 meters per second**	**Motion of the steel- plate at 0.2 meters per second**	**Motion of the steel- plate at 0.5 meters per second**
Nusselt number for mixture(liquid + vapor)	7572.304	5980.533	4695.833
Temperature Profile of Mixture(Liquid+Vapor) in Kelvin	818.7	861.2	941

It is clear from the graphical study that enhanced convection is indicated by a larger Nusselt number, especially under turbulent flow conditions. More specifically, as the plate moves at 0.1 metres per second, the mixture's convective heat transfer coefficient rises by 37.98%. The largest temperature decrease is seen on the plate moving at 0.1 metres per second, as seen in the above image. In these settings, a 13.1% drop in temperature is seen.

B. Heat flux of mixture for steel plate Motion at different Speeds

The provided data shows [table no.3] the heat flux experienced by a steel plate moving at different velocities: 0.1 meters per second, 0.2 meters per second, and 0.5 meters per second. The heat flux values are categorized into total mixture flux (combining liquid and vapor phases) and individual fluxes for phase-I (liquid) and phase-II (vapor). At 0.1 meters per second, the total heat flux for the mixture and phase-I are identical at 78,494,674.1 W/m², while phase-II contributes 321,069.652 W/m². As the plate velocity increases to 0.2 meters per second, both the total flux and phase-I flux increase to 96,541,094.3 W/m², with phase-II decreasing to 28,510.1139 W/m². At 0.5 meters per second, the total flux peaks at 132,309,040 W/m², with phase-I and phase-II fluxes reaching 132,309,040 W/m² and 57,309.343 W/m² respectively. These results indicate that as the plate velocity rises, the overall heat flux intensifies primarily due to increased liquid phase contribution, while the vapor phase's contribution remains comparatively minor across all velocities.below

Table No.3 Heat flux of mixture for steel plate Motion at different Speeds:

Heat flux	**Motion of the steel plate at 0.1 meters per second**	**Motion of the steel plate at 0.2 meters per second**	**Motion of the steel plate at 0.5 meters per second**
Heat flux for mixture	78494674.1	96541094.3	132309040
Heat flux for phase-I (liquid)	78494674.1	96541094.3	132309040
Heat flux for phase-II (vapor)	321069.652	28510.1139	57309.343

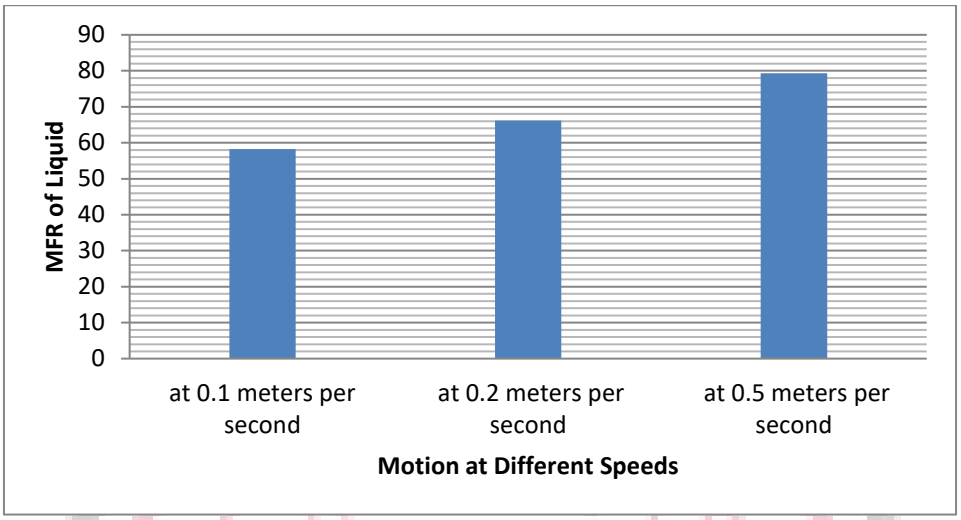

Figure 9. Variation of MFR for Liquid

The figure 9. Details the Mass Flow Rate (MFR) for liquid, on a steel plate at different velocities: 0.1 meters per second, 0.2 meters per second, and 0.5 meters per second. For the liquid phase, the MFR increases from 58.25 kg/sec at 0.1 m/s to 79.36096 kg/sec at 0.5 m/s.

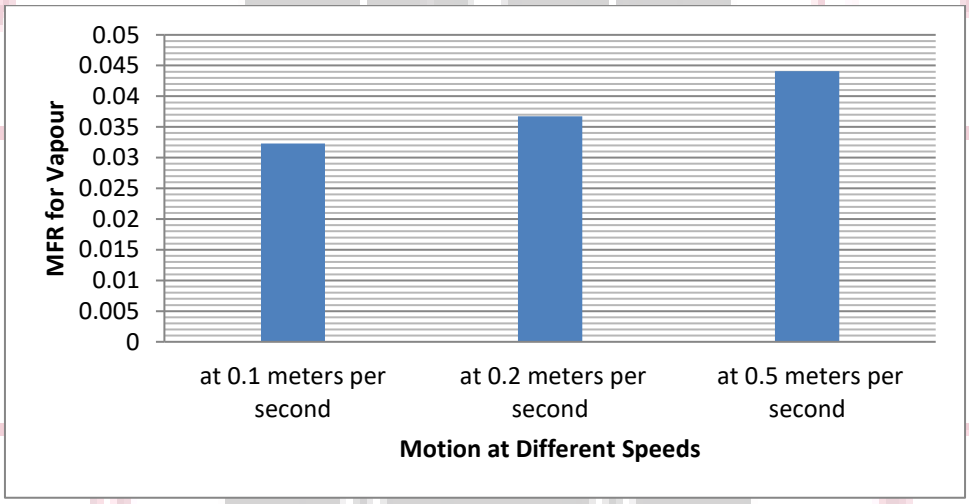

Figure10. Variation of MFR for Vapour

The figure10. details the Mass Flow Rate (MFR) for vapour, on a steel plate at different velocities: 0.1 meters per second, 0.2 meters per second, and 0.5 meters per second. The MFR for vapor rises from 0.0323 kg/sec at 0.1 m/s to 0.044069984 kg/sec at 0.5 m/s.

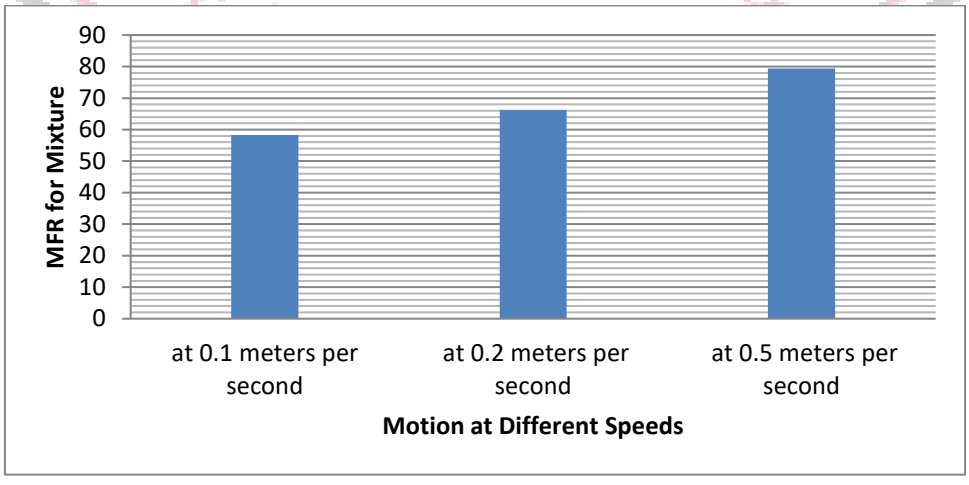

Figure 11.Variation of MFR for Mixture

Figure 11 shows the Mass Flow Rate for mixture on the steel plate for various velocity: 0.1 meters per second, 0.2 meters per second, and 0.5 meters per second. Their mixture MFRs merge to increase with an increasing plate velocity from 58.2629 kg/sec at 0.1 m/s to 79.376864 kg/sec at 0.5 m/s. These values show how the flow rates of liquid, vapor, and their combination have effects on the motion speed of the steel plate, changing the overall heat and mass transfer characteristics at the surface.

VI. CONCLUSION

Film boiling is one of the important events of heat transfer in industrial processes, particularly in applications such as cooling steel plates. This paper discusses research into the dynamics of film boiling on a moving steel plate using computational fluid dynamics, focusing on understanding property characteristics of heat transfer at various velocities. It is a volume of fluid model, which in turn captures the two-phase movement of liquid water interacting with vapor phases at the plate's surface. The results showed a high degree of variation in the temperature profile, Nusselt number, and heat flow at different speeds of the plate, for instance, 0.1, 0.2, and 0.5 m/s. It has been observed that, with an increase in the plate velocity, the convective heat transfer coefficient of the mixture decreases, indicating a decreasing overall heat dissipation efficiency with increasing speed. Phase-specific analysis brought out very clearly the complexity of film boiling under dynamic conditions, showing different patterns in heat fluxes and mass flow rates of liquid and vapor phases.

Such results can be utilized in optimizing cooling techniques, which are sure to increase the quality and optimality of industrial processes. Further studies on enhancing the possibility of heat transmission in film boiling conditions can focus on new materials and sophisticated cooling techniques. The use of these findings can also be extended to industries like steel manufacturing and other high-temperature operations that require effective heat dissipation. In summary, the current study contributes significantly to the unknown factors of film boiling dynamics on moving steel plates and underlines the requirement for developing tailored cooling strategies with regard to achieving high heat transfer in industrial heat transfer systems.

REFERENCES

[1] S. Kumar, A. Chaturvedi, A. Kumar, and C. Gupta, “Optimizing BLDC Motor Control in Electric Vehicles Using Hysteresis Current Controlled Boost Converters,” *Proc. - 2024 IEEE 16th Int. Conf. Commun. Syst. Netw. Technol. CICN 2024*, pp. 743–748, 2024, doi: 10.1109/CICN63059.2024.10847341.

[2] A. Kumar and S. Jain, “Critical Analysis on Multilevel Inverter Designs for,” vol. 14, no. 3, 2022, doi: 10.18090/samriddhi.v14i03.22.

[3] A. Kumar and S. Jain, “Enhancement of Power Quality with Increased Levels of Multi-level Inverters in Smart Grid Applications,” vol. 14, no. 4, pp. 1–5, 2022, doi: 10.18090/samriddhi.v14i04.07.

[4] C. B. Singh, A. Kumar, C. Gupta, S. Cience, T. Echnology, and D. C. Dc, “Comparative performance evaluation of multi level inverter for power quality improvement,” vol. 12, no. 2, pp. 1–7, 2024.

[5] A. Kumar and S. Jain, “Predictive Switching Control for Multilevel Inverter using CNN-LSTM for Voltage Regulation,” vol. 11, pp. 1–9, 2022.

[6] C. Gupta and V. K. Aharwal, “Design of Multi Input Converter Topology for Distinct Energy Sources,” *SAMRIDDHI*, vol. 14, no. 4, pp. 1–5, 2022, doi: 10.18090/samriddhi.v14i04.09.

[7] C. Gupta and V. K. Aharwal, “Design and simulation of Multi-Input Converter for Renewable energy sources,” *J. Integr. Sci. Technol.*, vol. 11, no. 3, pp. 1–7, 2023.

[8] C. Gupta and V. K. Aharwal, “Optimizing the performance of Triple Input DC-DC converter in an Integrated System,” *J. Integr. Sci. Technol.*, vol. 10, no. 3, pp. 215–220, 2022.

[9] A. Kumar and S. Jain, “Multilevel Inverter with Predictive Control for Renewable Energy Smart Grid Applications,” *Int. J. Electr. Electron. Res.*, vol. 10, no. 3, pp. 501–507, 2022, doi: 10.37391/IJEER.100317.

[10] S. Kumar, A. Kumar, C. Gupta, and A. Chaturvedi, “Future Trends in Fault Detection Strategies for DC Microgrid,” *Proc. - 2024 IEEE 16th Int. Conf. Commun. Syst. Netw. Technol. CICN 2024*, pp. 727–731, 2024, doi: 10.1109/CICN63059.2024.10847358.

[11] S. Kumar, A. Kumar, C. Gupta, A. Chaturvedi, and A. P. Tripathi, “Synergy of AI and PMBLDC Motors: Enhancing Efficiency in Electric Vehicles,” *IEEE Int. Conf. "Computational, Commun. Inf. Technol. ICCCIT 2025*, pp. 68–73, 2025, doi: 10.1109/ICCCIT62592.2025.10927757.

[12] B. B. Khatua, C. Gupta, and A. Kumar, “Harmonic Investigation Analysis of Cascade H Bridge Multilevel Inverter with Conventional Inverter using PSIM,” vol. 04, no. 03, pp. 9–14, 2021.

[13] R. Kumar and C. Gupta, “Methods for Reducing Harmonics in Wind Energy Conversion Systems : A Review I . Introduction II . Wind Energy Conversion System III . Harmonic Mitigation Methods,” vol. 04, no. 02, pp. 1–5, 2021.

[14] S. Khan, C. Gupta, and A. Kumar, “An Analysis of Electric Vehicles Charging Technology and Optimal Size Estimation,” vol. 04, no. 04, pp. 125–131, 2021.

[15] P. Ahirwar and C. Gupta, “Simulation of Continuous Mode Hybrid Power Station with Hybrid Controller,” vol. 03, no. 02, pp. 58–62, 2020.

[16] K. Jagwani, “Contemporary Technological Solutions towards fulfilment of Social Needs A Design Analysis of Energy Saving Through Regenerative Braking in Diesel Locomotive with Super-capacitors,” pp. 94–99, 2018.
[17] A. K. Singh and C. Gupta, “Controlling of Variable Structure Power Electronics for Self-Contained Photovoltaic Power Technologies,” vol. 05, no. 02, pp. 70–77, 2022.
[18] S. Kumar and A. Kumar, “Single Phase Seventeen Level Fuzzy-PWM Based Multicarrier Multilevel Inverter with Reduced Number of Switches.”
[19] A. Raj, A. Kumar, and C. Gupta, “Shunt Active Filters : A Review on Control Techniques II . Shunt Active Power Filter,” vol. 05, no. 02, pp. 78–81, 2022.
[20] Al-Nuaimi BT, Al-Mahdawi HK, Albadran Z, Alkattan H, Abotaleb M, El-kenawy E-SM. Solving of the Inverse Boundary Value Problem for the Heat Conduction Equation in Two Intervals of Time. Algorithms. 2023; 16(1):33. https://doi.org/10.3390/a16010033
[21] Varuvel, E. G., Sonthalia, A., Aloui, F., & Saravanan, C. G. (2023). Basics of heat transfer: Convection. In Handbook of Thermal Management Systems (pp. 35-77). Elsevier. https://doi.org/10.1016/B978-0-443-19017-9.00033-7
[22] Miroshnichenko, I. V., & Sheremet, M. A. (2023). Influence of Thermal Radiation on Heat Transfer through a Hollow Block. Journal of Applied and Computational Mechanics, 9(2), 419-429. https://doi.org/10.22055/jacm.2022.41759.3805
[23] Liu, X., Zou, Q., & Yang, R. (2022). Theoretical analysis of bubble nucleation in liquid film boiling. International Journal of Heat and Mass Transfer, 192, 122911. https://doi.org/10.1016/j.ijheatmasstransfer.2022.122911
[24] Stojanović, A. D., Belošević, S. V., Crnomarković, N. Đ., Tomanović, I. D., & Milićević, A. R. (2022). Nucleate pool boiling heat transfer: Review of models and bubble dynamics parameters. Thermal Science, 26(1 Part A), 157-174. https://doi.org/10.2298/TSCI200111069S
[25] Pati, A & Swain, Biswajit & Mohapatra, S. (2020). The Boiling Phenomena and their Proper Identification and Discrimination Methodology. Scientific Reports. 10. 10.1038/s41598-020-65342-0.
[26] Meena CS, Kumar A, Roy S, Cannavale A, Ghosh A. Review on Boiling Heat Transfer Enhancement Techniques. Energies. 2022; 15(15):5759. https://doi.org/10.3390/en15155759.
[27] Chen, H., Zhang, T., Gao, Q., Han, Z., Xu, Y., Yang, K., ... & Liu, X. (2022). Advance and prospect of power battery thermal management based on phase change and boiling heat transfer. Journal of Energy Storage, 53, 105254. https://doi.org/10.1016/j.est.2022.105254
[28] Kim, H., & Park, H. (2022). Bubble dynamics and induced flow in a subcooled nucleate pool boiling with varying subcooled temperature. International Journal of Heat and Mass Transfer, 183, 122054. https://doi.org/10.1016/j.ijheatmasstransfer.2021.122054.

inprotected.com